Received: 13 March 2019 | Revised: 22 July 2019 | Accepted: 30 November 2019

DOI: 10.1111/gbi.12375

ORIGINAL ARTICLE

gebiology WILEY

The evolving redox chemistry and bioavailability of vanadium in deep time

Eli K. Moore[1] | Jihua Hao[2] | Stephanie J. Spielman[3] | Nathan Yee[4,5]

[1]Department of Environmental Science, School of Earth and the Environment, Rowan University, Glassboro, NJ, USA

[2]University of Lyon, Université Lyon 1, Ens de Lyon, CNRS, Villeurbanne, France

[3]Department of Biological Sciences, College of Science and Mathematics, Rowan University, Glassboro, NJ, USA

[4]School of Biological and Environmental Sciences, Rutgers University, New Brunswick, NJ, USA

[5]Department of Earth and Planetary Sciences, Rutgers University, Piscataway, NJ, USA

Correspondence
Eli K. Moore, Department of Environmental Science, School of Earth and the Environment, Rowan University, Glassboro, NJ, USA.
Email: mooreek@rowan.edu

Funding information
National Aeronautics and Space Administration, Grant/Award Number: 80NSSC18M0093; French National Research Agency, Grant/Award Number: ANR-15-CE31-0010

Abstract

The incorporation of metal cofactors into protein active sites and/or active regions expanded the network of microbial metabolism during the Archean eon. The bioavailability of crucial metal cofactors is largely influenced by earth surface redox state, which impacted the timing of metabolic evolution. Vanadium (V) is a unique element in geo–bio-coevolution due to its complex redox chemistry and specific biological functions. Thus, the extent of microbial V utilization potentially represents an important link between the geo- and biospheres in deep time. In this study, we used geochemical modeling and network analysis to investigate the availability and chemical speciation of V in the environment, and the emergence and changing chemistry of V-containing minerals throughout earth history. The redox state of V shifted from a more reduced V(III) state in Archean aqueous geochemistry and mineralogy to more oxidized V(IV) and V(V) states in the Proterozoic and Phanerozoic. The weathering of vanadium sulfides, vanadium alkali metal minerals, and vanadium alkaline earth metal minerals were potential sources of V to the environment and microbial utilization. Community detection analysis of the expanding V mineral network indicates tectonic and redox influence on the distribution of V mineral-forming elements. In reducing environments, energetic drivers existed for V to potentially be involved in early nitrogen fixation, while in oxidizing environments vanadate (VO_4^{3-}) could have acted as a metabolic electron acceptor and phosphate mimicking enzyme inhibitor. The coevolving chemical speciation and biological functions of V due to earth's changing surface redox conditions demonstrate the crucial links between the geosphere and biosphere in the evolution of metabolic electron transfer pathways and biogeochemical cycles from the Archean to Phanerozoic.

KEYWORDS

bioavailability, deep time, geochemical modeling, mineral evolution network analysis, redox, vanadium

1 | INTRODUCTION

The utilization of metal cofactors in protein active sites played a central role in the evolution of biological electron transfer pathways and led to the expansion of the network of microbial metabolism in the Archean eon (Moore, Jelen, Giovannelli, Raanan, & Falkowski, 2017). Changing earth surface redox state, largely due to global oxygenation, affected the availability of different biologically crucial transition metals (Anbar & Knoll, 2002; Saito, Sigman, & Morel, 2003; Williams, 1981). Vanadium (V) is an intriguing metal in biology

Eli K. Moore and Jihua Hao contributed equally to this paper.

since it is an abundant dissolved transition metal in modern seawater with an approximate concentration of 30 nM, second only to Mo (100 nM; Rehder, 2008), but the biological utilization of V is more limited than other transition metal cofactors (Zerkle, House, & Brantley, 2005). Despite its limited biological use compared with other transition metals, V has several crucial functions for certain types of microbial communities: as an alternative cofactor in the nitrogen-fixing enzyme nitrogenase (McKenna, Benemann, & Traylor, 1970; Rehder, 2000), as a prosthetic group in haloperoxidases, as a primary electron acceptor in the form of vanadate (VO_4^{3-}; Lyalkova & Yurkova, 1992), and as phosphate mimicking enzyme inhibitor (Cantley et al., 1977).

It has been proposed that the function of V in biology evolved with the chemical differentiation of earth's surface environments, and similarly that vanadium's diverse redox chemistry may have made the element an important metal cofactor in electron transfer of primitive life-forms (Huang, Huang, Evans, & Glasauer, 2015; Rehder, 2008). The redox state of V is not only central to its biological function, but it is also linked to the evolution of the geosphere. V is recognized as an important redox tracer element because it exists in more redox states (II, III, IV, and V) than many other multi-valence elements in natural materials (Shearer, McKay, Papike, & Karner, 2006; Sutton et al., 2005). For example, in sedimentary systems, the incorporation of reduced V species (III and IV) in clays and other secondary minerals can be used as a redox indicator for past anoxic conditions (Gehring, Fry, Luster, & Sposito, 1994; Gehring, Schosseler, & Weidler, 1999; Lebedel et al., 2013). V(III) and V(IV) generated by low reduction potential will adsorb or complex with particulates, form insoluble hydroxides, and incorporate into minerals (Francois, 1988; Szalay & Szilágyi, 1967). In ancient rocks from the Archean eon, V partitioning into igneous rocks is linked to the redox state of the mantle (Canil, 1997), indicating that mantle-derived reduced volcanic gases H_2 and CO were not sufficient to support abiotic synthesis of biological precursor molecules (Canil, 2002).

The concentration of V in earth's crust is relatively low, but also more dispersed than other first row transition metals, resulting in rare concentrated mineral deposits (Reimann & Caritat, 1998). In fact, the majority of V minerals have been identified at only one or two localities (Liu et al., 2018). The study of V minerals has also increased the understanding of V geochemical cycling (Huang et al., 2015). Oxidative weathering of V(III)- and V(IV)-containing minerals to V(V) is a major mechanism of V mobilization in soil and sediment (Yang et al., 2014), but in the anoxic reducing conditions of the Archean eon, V would be expected to be insoluble and unavailable for biological utilization. As various mechanisms affect V availability, it remains largely unknown how the evolving geosphere impacted vanadium's redox state, aqueous geochemistry, and biological incorporation. For example, input of V to the ocean from weathering and rivers is partially removed by sea-floor vent-derived iron oxides (Trefry & Metz, 1989), but these processes may differ depending on earth surface redox conditions and tectonic regimes. New approaches using geochemical modeling and network analysis of mineral chemistry evolution provide a novel and robust approach to investigating the redox chemistry, chemical speciation, and bioavailability of V in deep time to understand this enigmatic element's place in the coevolution of the geo- and biospheres.

In this study, we investigated how changes in vanadium mineralogy and geochemistry over geologic time may have influenced V availability to the biosphere. We analyzed the distribution of vanadium minerals in each geologic eon and modeled the availability of V resulting from mineral weathering on the early earth. The analysis provides new insights into possible mineral sources of vanadium that were incorporated into the biosphere during the early stages of microbial evolution.

2 | METHODS

2.1 | Equilibrium calculations of V-O-H system under ambient conditions

The equilibrium constants for vanadium speciation diagrams were calculated with the Fortran computer code SUPCRT92b (Johnson, Oelkers, & Helgeson, 1992; Sverjensky, Hemley, & D'angelo, 1991). The equilibrium boundaries between the aqueous species and solids shown in the figures were calculated using their standard Gibbs free energies of formation (ΔG_f°) and corresponding activities of each aqueous species. The values of ΔG_f° were compiled from the literature and provided in Table S1. Considering the fact that metal hydroxides, instead of metal oxides, are primary sedimentary minerals and usually control the solubility of corresponding aqueous species under ambient conditions, we used vanadium hydroxides to calculate the equilibrium diagram.

2.2 | Solubility of vanadium minerals

The solubility limits of vanadium minerals described in this study were calculated by assuming the thermodynamic equilibrium of the mineral with corresponding dominant aqueous species under ambient conditions (Table 1, Table S1, Table S2). For example, the dominant aqueous species at Archean $pH_{2,g}$ and pH between 4 and 7 (typical pHs of weathering fluid) is VO^+ (Figure 1). We calculated the equilibrium constant (log K) of the reaction:

$$VO^+ + 2H_2O \rightleftarrows V(OH)_{3,s} + H^+$$

Provided a reasonable pH range (4–7) mimicking the acidity of weathering fluids, we can calculate the solubility of $V(OH)_{3,s}$ in Archean weathering fluid. Similarly, we calculated the solubility limits of vanadium sulfides (VS_s, $V_2S_{3,s}$, and $VS_{4,s}$) with the additional assumption that the concentration of H_2S_{aq} would be the dominant S species in acidic and moderately reducing fluid. The Archean atmosphere has low partial pressures of S gases (H_2S and SO_2) with mixing ratios less than 10^{-10} (Claire et al., 2014). Additionally, as Fe(II) is highly soluble in reducing Archean surface waters (Hao et al., 2017; Tosca et al., 2015), and the waters were probably S-poor

TABLE 1 Comparison of thermodynamic properties of V(II), Mn(II), and Fe(II) aqueous cations and crystal structure of the metal sulfide solids: Ionic radii ($r_{M^{2+}}$); Gibbs free energy of formation ($\Delta G_{f,M^{2+}}$); non-solvation Gibbs free energy ($\Delta G_{n,M^{2+}}$)

Divalent cation	$r_{M^{2+}}$ (Å)*	$\Delta G_{f,M^{2+}}$	$\Delta G_{n,M^{2+}}$
V	0.95[a]	−52.60[b]	72.70[c]
Mn	0.82[d]	−55.20[d]	81.26[d]
Fe	0.77[d]	−21.87[d]	119.17[d]
Metal(II) Sulfide	Structure	Space group	Crystallography[e]
V(II)S	Hexagonal	$P6_3mc$	a = 3.34 Å; b = 3.34 Å; c = 5.785 Å; Z = 2 α = 90°; β = 90°; γ = 120° V = 55.9 Å
Mn(II)S; rambergite	Hexagonal	$P6_3mc$	a = 3.982 Å; b = 3.982 Å; c = 6.445 Å; Z = 2 α = 90°; β = 90°; γ = 120° V = 88.503 Å^3
Fe(II)S; troilite	Hexagonal	$P6_3mc$	a = 5.9650 Å; b = 5.9650 Å; c = 11.7570 Å; Z = 12 α = 90°; β = 90°; γ = 120° V = 362.283 Å^3

Note: References

[a]Shannon (1976).

[b]Johnson and Nelson (2012).

[c]Calculated by this study using equation reported by Sverjensky and Molling (1992).

[d]Sverjensky and Molling (1992).

[e]Published data compiled by http://crystallography-online.com/ ("Crystal Structure Search" n.d.).

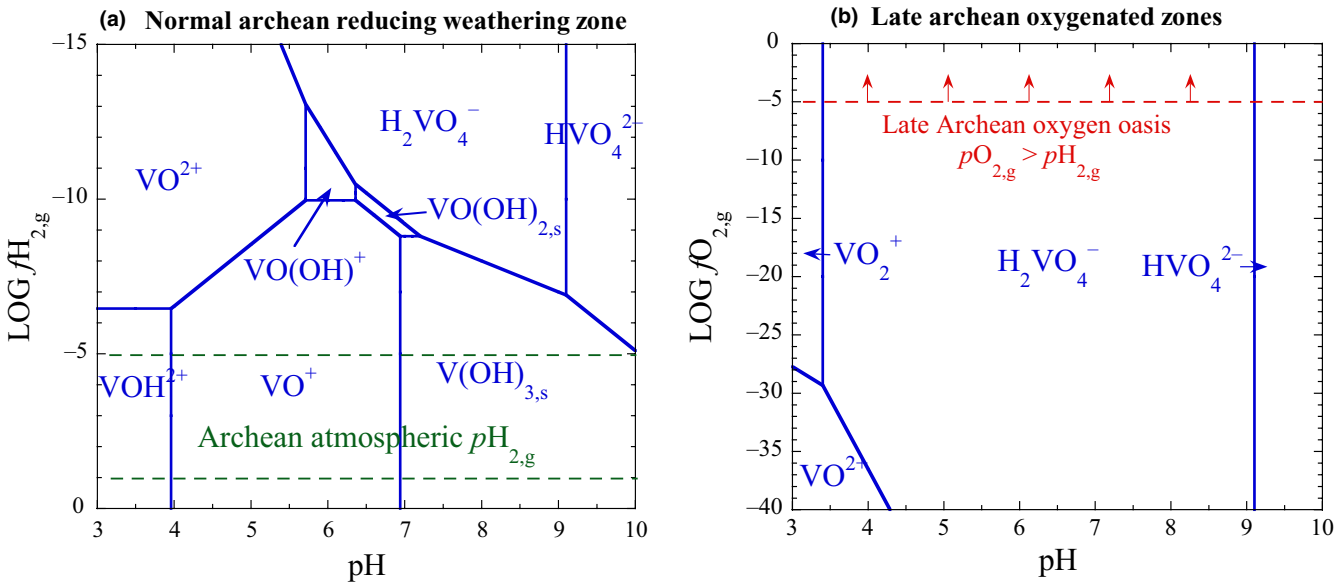

FIGURE 1 Equilibrium speciation of vanadium species and secondary minerals as a function of pH of weathering fluid in (a) reducing atmosphere where atmospheric level of $H_{2,g}$ surpasses levels of $O_{2,g}$ and controls the redox states of the surface environments; and (b) oxidizing atmosphere where the atmospheric level of $O_{2,g}$ surpasses levels of reducing gases and controls the redox states

controlled by the solubility of iron sulfides (Hao et al., 2017). In this study, we adopted c(H_2S,aq) = 10^{-7} mole/L as an approximation of soluble S(-II) in Archean weathering fluid (Hao et al., 2017). As a comparison, we also calculated the solubilities of vanadium sulfides at high concentrations of S, for example, c($H_2S_{,aq}$) = 10^{-3} mole/L, representing lower limits of the solubilities. Table S2 summarized all of the reactions used to calculate the solubilities and model assumptions.

2.3 | Vanadium mineral chemistry network analysis

Mineral chemistry, age, and oxidation state data for all known V-containing minerals were obtained from the Mineral Evolution Database (http://rruff.info/evolution/). Minerals were grouped by the redox state of V present in each mineral and plotted by age and mineral abundance to compare the emergence of different V redox states preserved in the mineral record in deep time. Bipartite

network construction, and subsequent Louvain community detection cluster analysis (Blondel, Guillaume, Lambiotte, & Lefebvre, 2008), of V mineral chemistry evolution was performed using the igraph package in R (Csardi & Nepusz, 2006). The two node types for the bipartite network are minerals and elements, such that network lines (referred to as edges) connect to the elements that compose each mineral (e.g., the chemical formula of coulsonite is FeV_2O_4; therefore, the coulsonite node has edge connections with Fe, V, and O). Four V mineral chemistry networks were created for all V-containing minerals: ≥4.0 Ga network representing the Hadean eon, asteroid, meteorite, and pre-solar sources (minerals >4.33 Ga are from asteroid, meteorite, or pre-solar sources); ≥2.5 Ga network representing the Archean and including all ≥4.0 Ga V minerals; ≥1.6 Ga network representing the Paleoproterozoic, and including all ≥2.5 Ga and ≥4.0 Ga V minerals; Present-day network including all V-containing minerals with known ages. Data wrangling was performed using R software, tidyverse package (Wickham, 2017). Regression analysis was performed using R software.

3 | RESULTS

3.1 | V weathering in the Archean Eon

The geochemical modeling results indicate that atmospheric levels of $H_{2,g}$ and weathering fluid pH are crucial determining factors in the speciation of aqueous vanadium and formation of secondary minerals (Figure 1a). The model results suggest that under the weakly reducing Archean redox conditions, V(III) is the only stable valence that can exist during weathering reactions. The dominant aqueous vanadium species in weathering fluids under Archean atmospheric $pH_{2,g}$ is VO^+ (occurring at pH 4–7). Under highly acidic conditions (below pH 4), VOH^{2+} would also contribute to vanadium mobilization. As the pH decreases by one unit at ambient conditions, the corresponding solubility of $V(OH)_{3,s}$ increases on average ten times. Conversely, at pH higher than neutral, trivalent vanadium is insoluble and will precipitate as $V(OH)_{3,s}$ or its dehydrated phase, $VO(OH)_s$ (montroseite). $VO(OH)_s$ is known as the primary mineral source of vanadium to form a wide range of V(III), V(IV), and V(V) oxides and hydroxides in modern oxidizing weathering processes (Evans & Garrels, 1958; Salminen et al., 2005). In acidic Archean weathering fluids (pH = 4–7; Hao et al., 2017), the calculated solubility of $V(OH)_{3,s}$ could reach 8.7×10^{-4} to 8.7×10^{-7} mole/L which is higher than the concentrations of dissolved V in modern river water (1.8×10^{-10} to 5.6×10^{-8} mole/L). Thus, the Archean weathering of V(III)-bearing minerals would have occurred under generally acidic leaching conditions, and acidic weathering fluids were capable of transporting considerable levels of dissolved vanadium as V(III). Currently, the concentration of V(III) in Archean river water is poorly constrained, but it should depend on various geologic and environmental factors such as the surface area of exposed land mass, V content in bedrock, precipitation, and elevation of land. Nevertheless, weathering of V(III)-bearing minerals such as $VO(OH)_s$ would have occurred under dominantly acidic leaching conditions of V(III) with negligible oxidation.

Our geochemical model also indicates that vanadium sulfides were highly soluble and weathered to form VO^+ at moderate pH, thus increasing the mobility of vanadium under S-poor Archean conditions. Using available thermodynamic properties of pure vanadium sulfides compiled from the literature (Table S1), we simulated the solubility of various vanadium sulfides (VS, V_2S_3, and VS_4) in reducing Archean surface waters. For example, under presumable Archean weathering conditions ($c(H_2S_{aq}) = 10^{-7}$ mole/L, pH = 6, and $p(H_{2,g}) = 10^{-5}$ bar), the solubilities of the crystalline solids VS_{cr}, $V_2S_{3,cr}$, and $VS_{4,cr}$ are higher than 1 mole/L. Even when $c(H_2S_{aq})$ is very high (10^{-3} mol/L), the solubilities of the vanadium sulfides are still higher than (10^{-3} mol/L). The calculated solubilities of vanadium sulfides are much higher than the solubility of $V(OH)_{3,s}$ (8.7×10^{-6} mole/L) and the highest concentration of vanadium reported in the modern river water (5.6×10^{-8} mole/L; Gaillardet et al., 2014). Therefore, vanadium sulfides are not a sink in the Archean vanadium geochemical cycle, but instead are potentially soluble sources if vanadium sulfides were present. However, vanadium could partially replace metals of similar geochemical properties in sulfide structures and found sulfide solid solutions, such as replacement of Fe(III) by V(III) (see Section 4 below).

Moreover, the modeling results indicate that the oxidized states (IV and V) of vanadium are not thermodynamically stable under Archean conditions (Figure 1a). In reducing surface waters containing reductants (e.g., $H_{2,aq}$, Fe^{2+}, and simple organics), weathering would be expected to reduce any available vanadium (IV and V) to vanadium (III). This would result in decreasing solubility of vanadium, but given the high solubility of V(III) in Archean river water, no V(III)-hydroxide would precipitate. Therefore, high valences of vanadium (IV and V) in Archean rocks would have been reduced during weathering, providing another source of vanadium for the early ocean and micro-organisms.

3.2 | Vanadium redox changes in minerals

There are three time periods in which the vast majority of V mineral maximum ages occur: 3.0–2.5 Ga, 2.1–1.7 Ga, and 0.7 Ga to present (Figure 2a). These three periods each correspond to the emergence of minerals that contain V in different redox states: from 3.0 to 2.5 Ga primarily V(III)-containing minerals emerged, from 2.1 to 1.7 Ga primarily V(V)-containing minerals emerged, and finally from 0.7 Ga to present minerals containing V(V), V(IV), and V(III) emerged (Figure 2b). The majority of V minerals with maximum ages in the 0.7 Ga to present period contain V(V), and all but two of the known V(IV) containing minerals also emerged in this period. Regression analysis shows that the redox state of V in V-containing minerals becomes more positive over time at an average rate of 0.18/billion years (p = .00021; Figure S1). The vast majority of vanadium minerals in the Archean are igneous at their maximum age locality, with only vanadinite ($Pb_5(VO_4)_3Cl$) occurring in a volcano-sedimentary setting

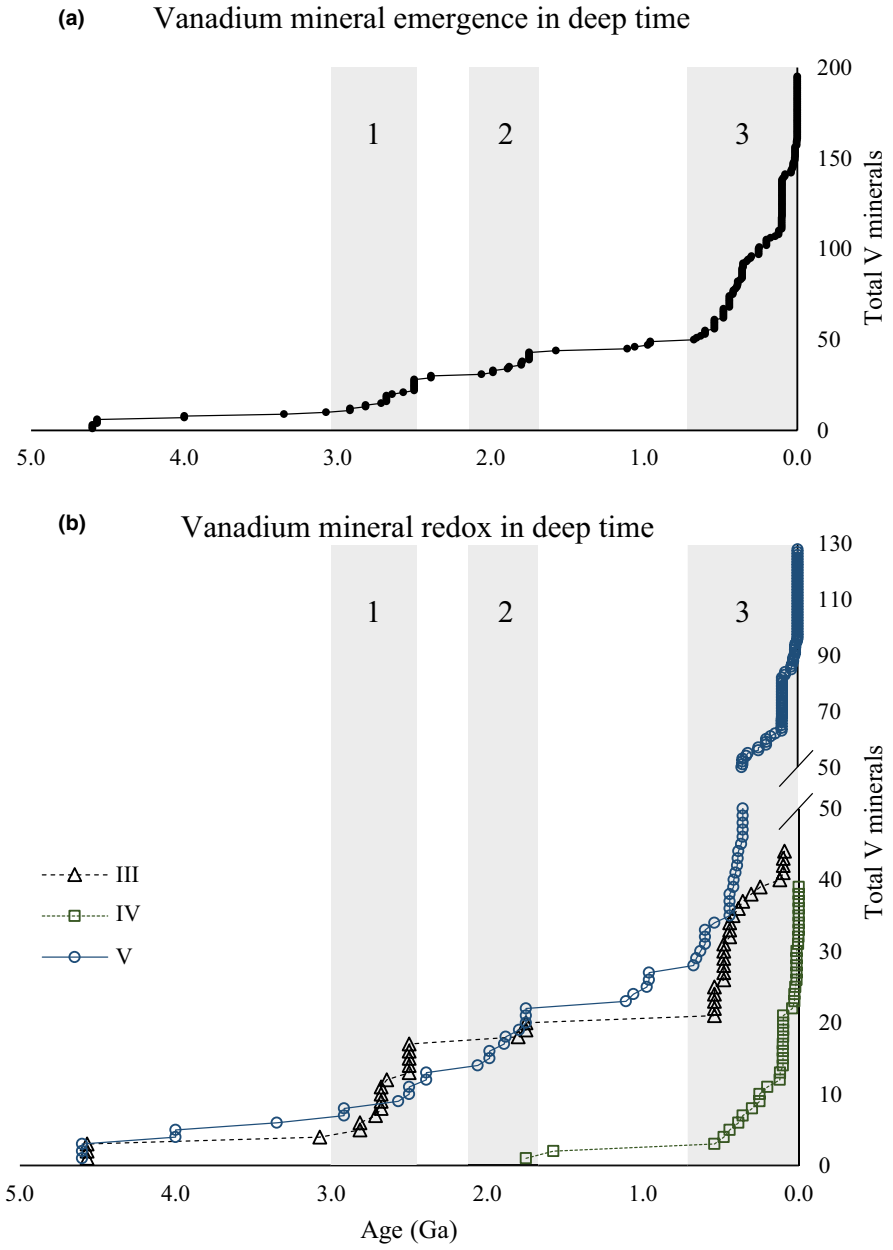

FIGURE 2 (a) Sum of vanadium (V) containing mineral species plotted by the maximum age in billions of years old (Ga). Minerals >4.33 Ga are from asteroid, meteorite, or pre-solar sources. Gray boxes indicate periods of enhanced V-containing mineral origination. (b) Sum of V-containing minerals plotted by maximum known age (Ga) separated by V redox state (III, IV, and V). Period I (3.0 to 2.5 Ga) is dominated by V(III) minerals; Period II (2.1 to 1.7 Ga) corresponds primarily to V(V) minerals; Period III (0.7 Ga to present) includes mostly V(V) minerals followed by V(IV) and V(III) minerals, respectively. The *y*-axis is rescaled at >50 V mineral species

at 3.35 Ga and mannardite ($Ba(Ti_6V_2)O_{16}$) occurring in a pulsed sedimentation greenstone detrital deposit at 3.07 Ga. In the Proterozoic and Phanerozoic, the majority of characterized V minerals are secondary in nature, occurring as products of weathering or hydrothermal alteration.

Network analysis illustrates that O and H are the most common mineral-forming elements associated with V throughout geologic time and thus the most centrally connected elements in the vanadium mineral chemistry network (Figure 3). Other than O and H; Al, Ca, Pb, and Cu are the only elements occurring in multiple vanadium minerals in Hadean, asteroid, meteorite, and pre-solar sources at ≥4.0 Ga (Figure 3a). At ≥2.5 Ga (Archean, Hadean, extraterrestrial), Ti, Fe, Al, Ca, Si, Pb, and Cu become increasingly important mineral-forming elements with V, all present in at least four V mineral species (Figure 3b). All other elements are components of three or fewer vanadium minerals at ≥2.5 Ga. In particular, the number of Ti-containing V minerals increases from 0 to 9 in the period of 4.0–2.5 Ga.

From the end of the Archean (2.5 Ga) to the end of the Paleoproterozoic (1.6 Ga), the number of V minerals that contain U (primarily U^{6+}) increase more than any element other than O or H (Figure 3c). In present day, the number of V minerals that contain Ca, Si, and Na increase more than any other elements besides O and H (Figure 3d). Separating mineral nodes by V redox state and then arranging the mineral nodes by maximum age shows that redox state is central in governing vanadium mineral formation (Figure 4). There are certain elements that only form minerals with V(V), other elements that only form minerals with V(III), and elements that form minerals with either V(V) and V(III) at >1.6 Ga (Figure 4). Louvain community detection cluster analysis (Blondel et al., 2008) of the >1.6 Ga V mineral chemistry network shows that clusters 1 and 5 include elements that primarily

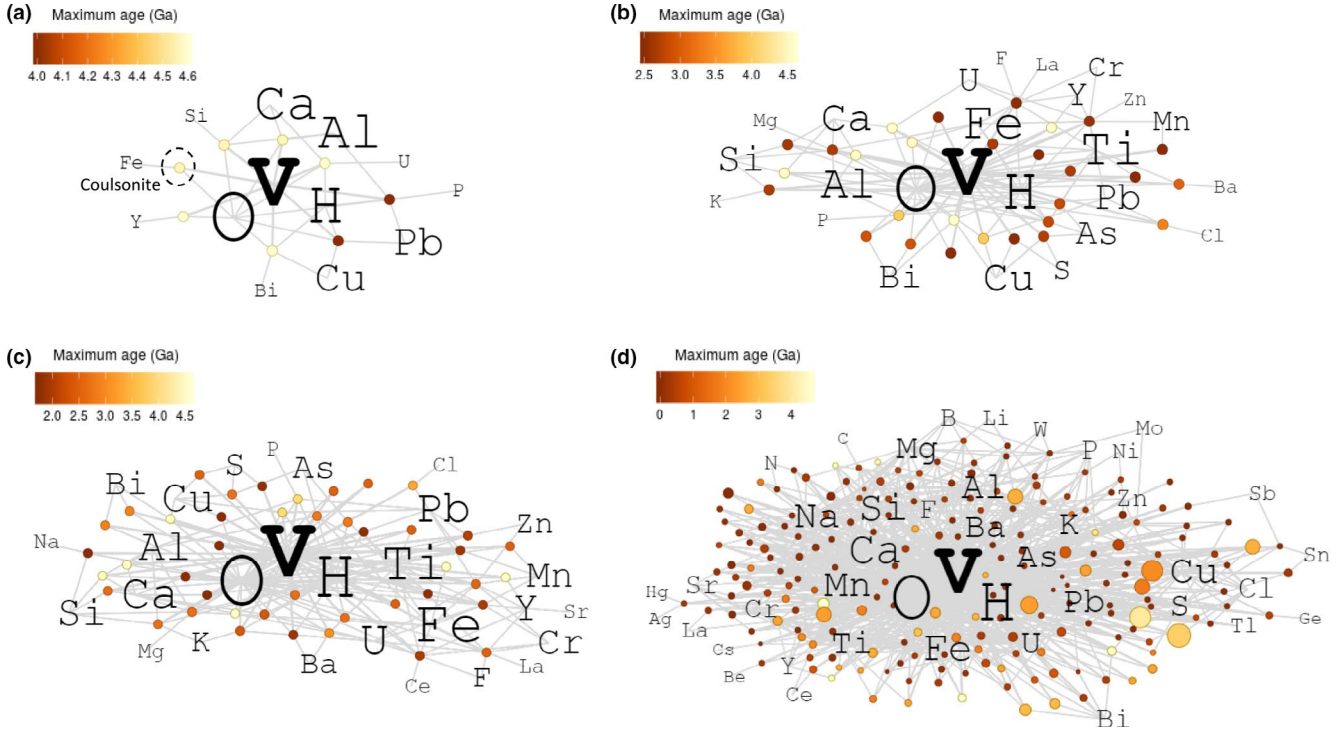

FIGURE 3 Evolving bipartite network of vanadium (V) containing minerals (circles) and the chemical elements that compose each mineral. Network lines (referred to as edges) connect minerals to the elements that compose them (e.g., the chemical formula of coulsonite is: FeV_2O_4, therefore the coulsonite node, circled in 3A, has edge connections with Fe, V, and O). Mineral nodes are colored by maximum known age (Ga). Chemical element nodes are sized by network degree (number of network edges). Networks contain minerals with maximum ages that occur at (a) ≥4.0 billion years ago (Ga) (includes asteroid, meteorite, and pre-solar sources >4.33 Ga); (b) ≥2.5 Ga; (c) ≥1.6 Ga; (d) present day (mineral nodes in 3D are sized by number of mineral localities). Each network contains all the minerals in the network time period that preceded it (e.g., The ≥2.5 Ga network contains all minerals from the ≥4.0 Ga network, etc.)

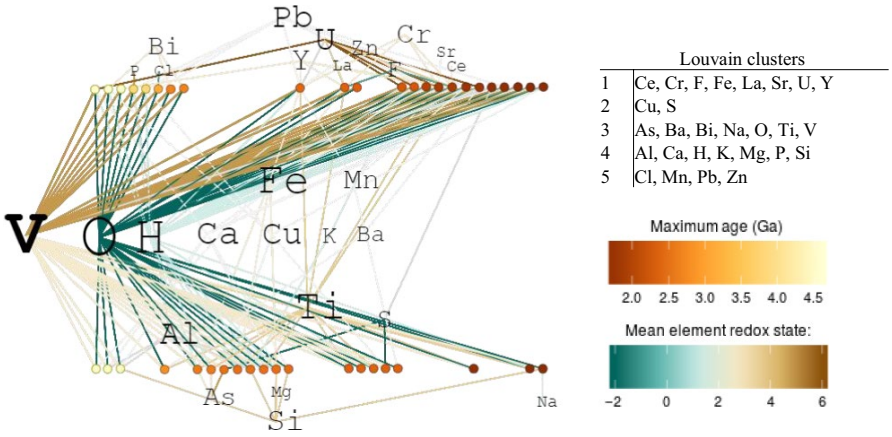

FIGURE 4 (a) Vanadium mineral chemistry timeline bipartite network containing all minerals with maximum ages ≥1.6 Ga. Minerals on the top of the network contain V(V), and minerals on the bottom of the network contain V(III). Mineral nodes are colored and sorted by maximum known age (Ga), and the network edges are colored by the redox state of the element in each mineral. Louvain community detection cluster analysis of chemical element nodes is shown in the embedded table

form minerals with V(V), while cluster 4 includes elements that primarily form minerals with V(III). Clusters 3 and 4 include the highly connected elements O, V, and H. Hydrogen primarily forms minerals with V(V) at >3.0 Ga, but then from 2.9 to 2.6 Ga primarily V(III) hydrogen minerals emerge (Figure 4).

In some cases, the number of minerals an element forms with V in deep time is not proportional to the number of minerals the same element forms with V at present day (Figure 5). Titanium (Ti) is present in a larger percentage of V minerals at 2.5, 1.6, and 0.7 Ga, but a smaller percentage at present day. Conversely, sulfur (S) and

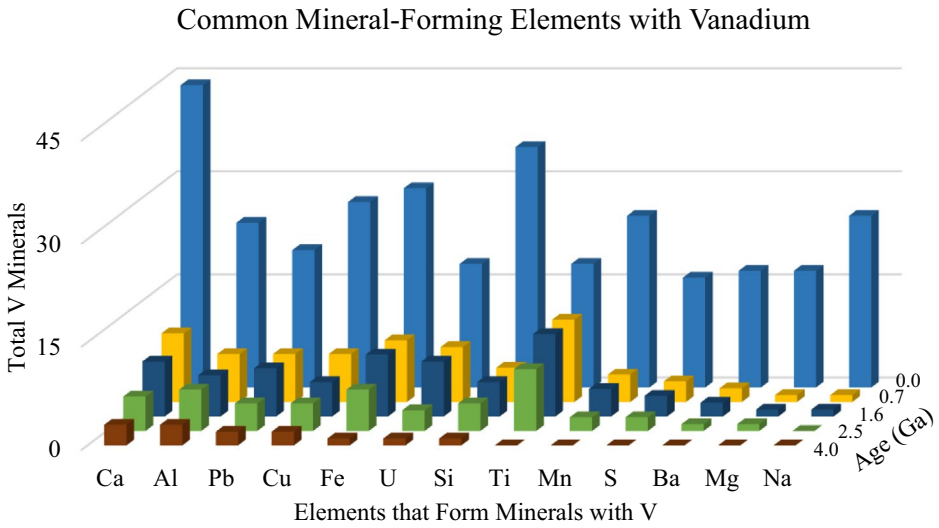

FIGURE 5 Abundance of common elements (excluding oxygen and hydrogen) that form minerals with vanadium (V) at ≥4.0 billion years ago (Ga) (includes asteroid, meteorite, and pre-solar sources >4.33 Ga); ≥2.5 Ga; ≥1.6 Ga; and present day

sodium (Na) are minor mineral-forming elements with V from 4.0 to 0.7 Ga, but both become important mineral-forming elements with V at <0.7 Ga to present day. Only three vanadium sulfide minerals have maximum known ages present at >0.541 Ga: colusite (2.716 Ga); sulvanite (2.5 Ga); patronite (1.8 Ga), all of which occur in volcanogenic massive sulfide deposits. All other vanadium sulfides with known maximum ages occur at ≤0.541 Ga, the majority of which are secondary minerals (sedimentary or hydrothermal alteration products).

4 | DISCUSSION

4.1 | Evolving vanadium redox state and availability

Our calculations indicate that solubility of V(III) minerals was not the limiting factor controlling the concentration of bioavailable vanadium in Archean waters. This result implies that the supply of vanadium was governed by continental weathering processes rather than mineral solubility. Recent studies indicate that the exposure of continental land above sea level is very limited until the middle of the Archean with lower elevation than that of the present-day plateaus (Bada & Korenaga, 2018; Flament, Coltice, & Rey, 2013; Korenaga, Planavsky, & Evans, 2017), thus possibly constraining the input of continental weathering of vanadium to the shallow ocean. Additionally, pervasive hydrothermal flux of Fe (Kump & Seyfried, 2005) and massive precipitation of iron (hydr)oxides as banded iron formations (BIFs; Klein, 2005) further limited the availability of vanadium in early seawater as surface adsorption or coprecipitation of vanadium along with iron (hydr)oxides and clay minerals are major sinks of the modern vanadium cycle (Breit & Wanty, 1991; Huang et al., 2015; Schlesinger, Klein, & Vengosh, 2017), and presumably in the Archean. Therefore, before the prominent occurrence and elevation of continental lands in the mid-Archean, limited weathering supply and large adsorption/coprecipitation sinks would have resulted in low concentrations of vanadium in the oceans, as evidenced by low V concentrations in early Archean BIFs (Aoki, Kabashima, Kato, Hirata, & Komiya, 2018).

Our thermodynamic calculations indicate that pentavalent vanadium is stable in late Archean oxygen oases and after the eventual oxygenation of the atmosphere at 2.33 Ga (Farquhar, Bao, & Thiemens, 2000; Luo et al., 2016) (Figure 1b). Because V(V) has a higher solubility than V(III) and V(IV) (Huang et al., 2015), the formation of oxidovanadates(V) would have increased the concentrations of vanadium in the environment. We calculated the solubility of several secondary vanadium minerals that control the solubility of vanadium (III, IV, and V) in surface waters under either reducing or oxidizing conditions. Our results suggest that the order of solubility as V(III) (solubility of $V(OH)_{3,s}$ is 8.7×10^{-6} mole/L at pH = 6) ≈ V(IV) (solubility of $VO(OH)_{2,s}$ is 2.2×10^{-6} mole/L at pH 6) « V(V) (solubility of $Ca(VO_3)_{2,s}$ is 1.4×10^{-3} mole/L at pH = 6; Table S2). In addition, under oxidizing conditions, weathering of sulfide minerals could acidify the weathering fluid, increasing solubility (Figure 1; Table S2) and facilitating the dissolution rates of vanadium minerals (Hu, Yue, & Peng, 2018). Moreover, continental land exposed above sea level in the end of the Archean was greater than in the early and middle Archean (Flament et al., 2013; Korenaga et al., 2017) resulting in greater continental weathering.

Progressive increase of V content in BIFs from the Mesoarchean to the Proterozoic (Aoki et al., 2018) and black shale pyrite in late Archean and Paleoproterozoic (Large et al., 2014) are coherent with an elevated influx of vanadium to the early ocean by oxidative weathering and riverine transport. The presence of oxidized vanadium is also observed by the preservation of V(V) minerals emerging in the Proterozoic and continuing into the Phanerozoic (Figure 2b). The average V content of the upper continental crust did not change very much throughout earth history (tables 3 and 4 of Condie, 1993); therefore, the evolution of crustal V content had a relatively minor effect on the evolution of continental delivery of V compared with

the impact of changing atmospheric redox conditions and $pCO_{2,g}$. The increase in V concentration in ocean water due to expanded oxidizing conditions is similar to geochemical models and sedimentary records indicating that the concentration of Mo, Ni, Zn, and Cu increased with ocean oxygenation (Canfield, 1998; Saito et al., 2003; Zerkle et al., 2005; Scott et al., 2008; Anbar, 2008; Hardisty et al., 2014). The same models and sedimentary records show that Fe, Mn, and Co concentrations decreased in ocean water due to marine oxygenation, and that the concentrations of most of these metals (Ni, Zn, Cu, Fe, Mn, and Co) decreased due to H_2S rich conditions of the Proterozoic.

4.2 | Vanadium chemistry preserved in the mineral record

Vanadium mineral chemistry network analysis, linear regression, and geochemical modeling show that the redox state and speciation of V changed in deep time with changing planetary redox conditions (Figures 1 and 2; Figure S1). In the reducing conditions of the Archean Eon (4.0–2.5 Ga), vanadium existed in more reduced states relative to the Proterozoic and Phanerozoic, which contributed to the preservation of V(III) minerals from 3.0 to 2.5 Ga. Under oxidizing conditions after the Great Oxidation Event (GOE), enhanced V(V) mineral formation and preservation occurred at 2.1–1.7 Ga followed by extensive V(V) and V(IV) mineral formation and preservation 0.7 Ga to present day. The clustering of V mineral-forming elements reflected these redox changes along with apparent tectonic processes, similar to V mineral clustering by locality described by Liu et al. (2018). The redox state of emerging V minerals responds differently to planetary oxygenation than other proxies, such as redox sensitive metals Mo and Re (Anbar et al., 2007) or ^{15}N fractionation (Godfrey & Falkowski, 2009). The timing of the beginning of the rise of V(V) and V(IV) mineral maximum known ages at approximately 0.7 Ga (Figure 2b; Figure S1) coincides more closely with the oxidation of manganese preserved in the mineral record (Hazen et al., 2019; Hummer et al., 2017) and the development of oxygenated deep ocean waters at 1.0–0.54 Ga, as proposed by Canfield (Canfield, 1998).

Our analysis of the expanding V mineral network indicates tectonic and redox influence on the distribution of V mineral-forming elements. Plate tectonic convergences are important events for mineral formation (Hazen et al., 2008), and the timing of the onset of plate tectonics has been strongly debated in recent decades (Cawood, Kröner, & Pisarevsky, 2006; Hopkins, Harrison, & Manning, 2010; Korenaga, 2013; Stern, 2005). A recent review by Cawood et al. (2018) presents multiple lines of evidence that significant changes to the earth's tectonic processes took place between 3.2 and 2.5 Ga. The V mineral origination Period I (Figure 2) may be a result of emerging tectonic processes at this time period. Indeed, the V minerals with maximum ages that occur during Period I (3.0–2.5 Ga) primarily occur in igneous or volcanic settings. Reducing conditions would have also contributed to the emergence and preservation of reduced V(III) minerals in the Archean (Figure 1). Period II (2.1–1.7 Ga) includes comparably more V minerals located in volcano-sedimentary settings, potentially indicating changing tectonic and preservation processes (Table S3). The changes in V mineral chemistry in deep time, particularly related to redox state and the incorporation of hydrogen, are likely influenced by the exclusive presence of meteoritic sources at >4.0 Ga, the transition to massive volcanic sulfide deposits and igneous sources from 4.0 to 2.9 Ga, evolving tectonic processes that resulted in porphyry development and involvement of water in mineral formation from 2.9 to 2.6 Ga, and finally the expanding oxidizing conditions from <2.5 to 1.6 Ga (Figures 1, 2 and 4; Table S3). The elements V and Al have a strong association in geologic time evidenced by the common substitution of V for Al in clays, particularly illite and muscovite (Meunier, 1994; Pan & Fleet, 1992; Zheng et al., 2017). Al is also an important mineral-forming element with V throughout the mineral record, forming minerals predominately with V(III) at ≥1.6 Ga and increasingly with V(V) and V(IV) at <1.6 Ga (Figures 3 and 4).

There is a general trend in the Mineral Evolution Database (http://rruff.info/evolution/) of preserved pulses of mineralization during episodes of continental assembly which initiate mineral formation and preservation in the cores of resulting mountain ranges (Hazen et al., 2019). Indeed, these periods of continental assembly coincide with periods 1, 2, and 3 of V mineral origination (Figure 2). Additionally, due to the nature of plate tectonics, there is a greater probability that older rocks and minerals will be subducted and lost to the mantle (Rapp & Watson, 1995; Taylor & McLennan, 1995), resulting in preservation and sampling bias for minerals that occur at ≤0.7 Ga. Mineral-forming elements associated with V can also affect weathering and preservation. For example, titanium is highly immobile and readily forms Ti-oxides and Fe-Ti hydroxides during weathering processes (Nesbitt, 1979), thereby resulting in a high proportion of Ti-containing vanadium minerals preserved compared with other mineral-forming elements from 2.5 to 0.7 Ga (i.e., 67% of modern day Ti-containing vanadium minerals were preserved at 0.7 Ga; Figure 5). By contrast, Na-containing vanadium minerals are more susceptible to chemical weathering (Middelburg, van der Weijden, & Woittiez, 1988), and thus make up a very small percentage of present-day Na-containing V minerals are preserved at ≥0.7 Ga (Figure 5). Furthermore, strong oxidizing conditions at <0.7 Ga also likely contributed to the formation of V minerals with Na, alkaline earth metals (Ca, Mg, and Ba), and silicates (Hazen et al., 2008). The greater presence of primary sedimentary V minerals at <0.7 Ga and primarily igneous/metamorphic V minerals ≥0.7 Ga (http://rruff.info/evolution/) suggests that weathering and lack of mineral preservation could have been a source of V to the environment in the Archean and Proterozoic eons. The fact that only 5 vanadium sulfide minerals are preserved at ≥0.1 Ga (http://rruff.info/evolution/) also supports our modeled result that sulfides were a source of V to the environment in the Archean and Proterozoic.

4.3 | Biological implications of deep time vanadium redox

Energetic drivers potentially existed in the reducing conditions of the early Archean for V to be involved in early nitrogen fixation including the reduction of N_2 gas by V(II) in laboratory experimentation (Shilov et al., 1971), greater energetic efficiency by V-nitrogenase than Mo-nitrogenase at lower temperatures (Miller & Eady, 1988), and Mo limitation in the early Archean ocean due to low weathering input and scavenging by sulfides (Anbar, 2008; Saito et al., 2003; Scott et al., 2008; Zerkle et al., 2005). Greater solubility of vanadium sulfides than molybdenum sulfides suggests that V-nitrogenase could have been an evolutionary intermediate between Fe-nitrogenase and Mo-nitrogenase (Zerkle, House, Cox, & Canfield, 2006). Incorporation of V(II) into sulfide structures would be expected to be similar to Mn(II) (Table 1), which is known to form various Mn-sulfide structures. Evidence of an ancient origin for V-nitrogenase is also apparent in the capability of V-nitrogenase in *Azotobacter vinelandii* to reduce carbon monoxide (abundant in the early Archean atmosphere) to the hydrocarbons ethylene (C_2H_2), ethane (C_2H_6), and propane (C_3H_8; Lee, Hu, & Ribbe, 2010). Further study is needed to investigate role of V in early nitrogen fixation.

The two modern predominant forms of vanadium in the geosphere and biosphere that are available to microbial utilization under modern oxic conditions are soluble vanadate (VO_4^{3-}) and insoluble oxidovanadium (VO^{2+}, a.k.a. vanadyl; Rehder, 2008). Based on our modeling results, $H_2VO_4^-$ (which dissociates to VO_4^{3-}) would be more abundant in Archean oxygen oases, while VO^{2+} would only occur in low oxygen low pH conditions (Figure 1b). Vanadate is a primary electron acceptor for various microbes (Antipov, Lyalikova, Khijniak, Nikolay, & L'vov, 1998; Carpentier, Smet, Beeumen, & Brigé, 2005; Ortiz-Bernad, Anderson, Vrionis, & Lovley, 2004; Lyalkova & Yurkova, 1992), primarily resulting in the production of vanadyl ($H_2V(V)O_4^-/V(IV)O^{2+}$ redox couple potential = +340 mV; Rehder, 2008). *Pseudomonas* bacteria can use multiple organic electron donors, carbon monoxide (CO), or dihydrogen (H_2) as the electron source in vanadate reduction (Lyalkova & Yurkova, 1992).

In addition to its function as a primary electron acceptor, vanadate can also act as an enzyme inhibitor. Vanadate has similar structural features to phosphate, and vanadate can thus easily substitute for phosphate in enzymes such as phosphatases and kinases (Rehder, 2015), which inhibits the enzyme (Cantley et al., 1977; Chasteen, 1995). Conversely, phosphate inhibits vanadate reduction in *Shewanella oneidensis* (Carpentier et al., 2003). Sequence alignment and crystal structure analysis of vanadium haloperoxidases has revealed that amino acids that bind the vanadate cofactor are conserved with a family of acid phosphatases (Hemrika, Renirie, Dekker, Barnett, & Wever, 1997; Littlechild, Garcia-Rodriguez, Dalby, & Isupov, 2002; Wever & Hemrika, 2001). Recently, it has been shown that an increase in arsenate (AsO_4^{3-}) in marine shales after 2.45 Ga represented the establishment of an oxidative component to the arsenic cycle and the presence of toxic arsenate in seawater (Fru et al., 2019). A rise in dissolved vanadate after the GOE follows this trend of selective pressures against microbial communities in the form of oxidized elements.

5 | CONCLUSIONS

Vanadium is an intriguing enigmatic element for study in geobiological context due to its complex redox chemistry that affects chemical speciation, mineralogy, availability, and biological functions. The redox state of V shifted from a more reduced V(III) state in Archean aqueous geochemistry and mineralogy to more oxidized V(V) and V(IV) states in the Proterozoic and Phanerozoic. The weathering of vanadium sulfides, vanadium alkali metal minerals, and vanadium alkaline earth metal minerals were likely important sources of V to the environment and for microbial utilization. Community detection analysis of the expanding V mineral chemistry network indicates tectonic processes and redox influenced the distribution of V mineral-forming elements, particularly, H, Si, Pb, and U. In reducing environments, energetic drivers existed for V to potentially be involved in early nitrogen fixation, while in oxidizing environments, vanadate (VO_4^{3-}) acted as a metabolic electron acceptor and phosphate mimicking enzyme inhibitor. The expanding biological functions of V due to earth's changing surface redox conditions demonstrate the crucial links between the geosphere and biosphere in the evolution of metabolic electron transfer pathways and expanding biogeochemical cycles from the Archean to Phanerozoic.

ACKNOWLEDGMENTS

We acknowledge NASA Astrobiology Institute for funding, Grant Number: 80NSSC18M0093; Proposal: ENIGMA: EVOLUTION OF NANOMACHINES IN GEOSPHERES AND MICROBIAL ANCESTORS (NASA ASTROBIOLOGY INSTITUTE CYCLE 8). Funding support for J. Hao is from the French National Research Agency through the PREBIOM (Primitive Earth—Biomolecules Interacting with Hydrothermal Oceanic Minerals) project no. ANR-15-CE31-0010. We also acknowledge Josh Golding at the University of Arizona for data support with the Mineral Evolution Database (http://rruff.info/ima/).

ORCID

Eli K. Moore https://orcid.org/0000-0002-9750-7769
Jihua Hao https://orcid.org/0000-0003-3657-050X
Stephanie J. Spielman https://orcid.org/0000-0002-9090-4788
Nathan Yee https://orcid.org/0000-0002-1023-5271

REFERENCES

Anbar, A. D. (2008). Elements and evolution. *Science*, *322*(5907), 1481–1483. https://doi.org/10.1126/science.1163100

Anbar, A. D., Duan, Y., Lyons, T. W., Arnold, G. L., Kendall, B., Creaser, R. A., … Buick, R. (2007). A whiff of oxygen before the great oxidation event? *Science*, *317*(5846), 1903–1906. https://doi.org/10.1126/science.1140325

Anbar, A. D., & Knoll, A. H. (2002). Proterozoic ocean chemistry and evolution: A bioinorganic bridge? *Science*, *297*(5584), 1137–1142. https://doi.org/10.1126/science.1069651

Antipov, A. N., Lyalikova, N. N., Khijniak, T. V., & L'vov, N. P. (1998). Molybdenum-free nitrate reductases from vanadate-reducing bacteria. *FEBS Letters*, *441*(2), 257–260. https://doi.org/10.1016/S0014-5793(98)01510-5

Aoki, S., Kabashima, C., Kato, Y., Hirata, T., & Komiya, T. (2018). Influence of contamination on banded iron formations in the isua supracrustal belt, west Greenland: Reevaluation of the eoarchean seawater compositions. *Geoscience Frontiers*, *9*(4), 1049–1072. https://doi.org/10.1016/j.gsf.2016.11.016

Bada, J. L., & Korenaga, J. (2018). Exposed areas above sea level on earth %3e3.5 Gyr ago: Implications for prebiotic and primitive biotic chemistry. *Life*, *8*(4), 55. https://doi.org/10.3390/life8040055

Blondel, V. D., Guillaume, J.-L., Lambiotte, R., & Lefebvre, E. (2008). Fast unfolding of communities in large networks. *Journal of Statistical Mechanics: Theory and Experiment*, *2008*(10), P10008. https://doi.org/10.1088/1742-5468/2008/10/P10008

Breit, G. N., & Wanty, R. B. (1991). Vanadium accumulation in carbonaceous rocks: A review of geochemical controls during deposition and diagenesis. *Chemical Geology*, *Trace Metals in Petroleum Geochemistry*, *91*(2), 83–97. https://doi.org/10.1016/0009-2541(91)90083-4

Canfield, D. E. (1998). A new model for Proterozoic ocean chemistry. *Nature*, *396*(6710), 450–453. https://doi.org/10.1038/24839

Canil, D. (1997). Vanadium partitioning and the oxidation state of Archaean komatiite magmas. *Nature*, *389*(6653), 842–845. https://doi.org/10.1038/39860

Canil, D. (2002). Vanadium in peridotites, mantle redox and tectonic environments: Archean to present. *Earth and Planetary Science Letters*, *195*(1), 75–90. https://doi.org/10.1016/S0012-821X(01)00582-9

Cantley, L. C., Josephson, L., Warner, R., Yanagisawa, M., Lechene, C., & Guidotti, G. (1977). Vanadate is a potent (Na, K)-ATPase inhibitor found in ATP derived from muscle. *Journal of Biological Chemistry*, *252*(21), 7421–7423.

Carpentier, W., De Smet, L., Van Beeumen, J., & Brigé, A. (2005). Respiration and growth of shewanella oneidensis MR-1 using vanadate as the sole electron acceptor. *Journal of Bacteriology*, *187*(10), 3293–3301. https://doi.org/10.1128/JB.187.10.3293-3301.2005

Carpentier, W., Sandra, K., De Smet, I., Brigé, A., De Smet, L., & Van Beeumen, J. (2003). Microbial reduction and precipitation of vanadium by shewanella oneidensis. *Applied and Environment Microbiology*, *69*(6), 3636–3639. https://doi.org/10.1128/AEM.69.6.3636-3639.2003

Cawood, P. A., Hawkesworth, C. J., Pisarevsky, S. A., Bruno, D., Capitanio, F. A., & Oliver, N. (2018). Geological archive of the onset of plate tectonics. *Philosophical Transactions of the Royal Society A: Mathematical, Physical and Engineering Sciences*, *376*(2132), 20170405. https://doi.org/10.1098/rsta.2017.0405

Cawood, P. A., Kröner, A., & Pisarevsky, S. (2006). Precambrian plate tectonics: Criteria and evidence. *GSA Today*, *16*, 4–11. https://doi.org/10.1130/GSAT01607.1

Chasteen, N. (1995). *Metal ions in biological systems* (Vol. *31*). In H. Sigel, & A. Sigel (Eds.). New York, NY: Marcel Dekker Inc.

Condie, K. C. (1993). Chemical composition and evolution of the upper continental crust: Contrasting results from surface samples and shales. *Chemical Geology*, *104*(1), 1–37. https://doi.org/10.1016/0009-2541(93)90140-E

Csardi, G., & Nepusz, T. (2006). The Igraph software package for complex network research. *InterJournal*, *Complex Systems*, *1695*(5), 1–9.

Evans, H. T., & Garrels, R. M. (1958). Thermodynamic equilibria of vanadium in aqueous systems as applied to the interpretation of the Colorado plateau ore deposits. *Geochimica et Cosmochimica Acta*, *15*(1), 131–149. https://doi.org/10.1016/0016-7037(58)90015-2

Farquhar, J., Bao, H., & Thiemens, M. (2000). Atmospheric influence of earth's earliest sulfur cycle. *Science*, *289*(5480), 756–758. https://doi.org/10.1126/science.289.5480.756

Flament, N., Coltice, N., & Rey, P. F. (2013). The evolution of the 87Sr/86Sr of marine carbonates does not constrain continental growth. *Precambrian Research*, *Evolving Early Earth*, *229*(May), 177–188. https://doi.org/10.1016/j.precamres.2011.10.009

Francois, R. (1988). A study on the regulation of the concentrations of some trace metals (Rb, Sr, Zn, Pb, Cu, V, Cr, Ni, Mn and Mo) in saanich inlet sediments, British Columbia, Canada. *Marine Geology*, *83*(1), 285–308. https://doi.org/10.1016/0025-3227(88)90063-1

Fru, E. C., Somogyi, A., El Albani, A., Medjoubi, K., Aubineau, J., Robbins, L. J., … Konhauser, K. O. (2019). The rise of oxygen-driven arsenic cycling at ca. 2.48 Ga. *Geology*, *47*(3), 243–246. https://doi.org/10.1130/G45676.1

Gehring, A. U., Fry, I. V., Luster, J., & Sposito, G. (1994). Vanadium in sepiolite: A redox-indicator for an ancient closed brine system in the Madrid Basin, Central Spain. *Geochimica et Cosmochimica Acta*, *58*(16), 3345–3351. https://doi.org/10.1016/0016-7037(94)90090-6

Gehring, A. U., Schosseler, P. M., & Weidler, P. G. (1999). Mineral formation and redox-sensitive trace elements in a near-surface hydrothermal alteration system. *Geochimica et Cosmochimica Acta*, *63*(13), 2061–2069. https://doi.org/10.1016/S0016-7037(99)00134-9

Godfrey, L. V., & Falkowski, P. G. (2009). The cycling and redox state of nitrogen in the Archaean Ocean. *Nature Geoscience*, *2*(10), 725–729. https://doi.org/10.1038/ngeo633

Hardisty, D. S., Zunli, L. U., Planavsky, N. J., Bekker, A., Philippot, P., Zhou, X., & Lyons, T. W. (2014). An iodine record of paleoproterozoic surface ocean oxygenation. *Geology*, *42*(7), 619–622. https://doi.org/10.1130/G35439.1

Hazen, R. M., Downs, R. T., Eleish, A., Fox, P., Gagné, O. C., Golden, J. J., … Zhong, H. (2019). Data-driven discovery in mineralogy: Recent advances in data resources, analysis, and visualization. *Engineering*, *5*(3), 397–405. https://doi.org/10.1016/j.eng.2019.03.006

Hazen, R. M., Papineau, D., Bleeker, W., Downs, R. T., Ferry, J. M., McCoy, T. J., … Yang, H. (2008). Mineral Evolution. *American Mineralogist*, *93*(11–12), 1693–1720. https://doi.org/10.2138/am.2008.2955

Hemrika, W., Renirie, R., Dekker, H. L., Barnett, P., & Wever, R. (1997). From phosphatases to vanadium peroxidases: A similar architecture of the active site. *Proceedings of the National Academy of Sciences of the United States of America*, *94*(6), 2145–2149. https://doi.org/10.1073/pnas.94.6.2145

Hopkins, M. D., Mark Harrison, T., & Manning, C. E. (2010). Constraints on hadean geodynamics from mineral inclusions in >4Ga zircons. *Earth and Planetary Science Letters*, *298*(3), 367–376. https://doi.org/10.1016/j.epsl.2010.08.010

Hu, X., Yue, Y., & Peng, X. (2018). Release kinetics of vanadium from vanadium (III, IV and V) oxides: Effect of PH, temperature and oxide dose. *Journal of Environmental Sciences*, *67*(May), 96–103. https://doi.org/10.1016/j.jes.2017.08.006

Huang, J.-H., Huang, F., Evans, L., & Glasauer, S. (2015). Vanadium: global (bio)geochemistry. *Chemical Geology*, *417*(December), 68–89. https://doi.org/10.1016/j.chemgeo.2015.09.019

Hummer, D. R., Golden, J. J., Hystad, G., Downs, R. T., Eleish, A., Liu, C., …Hazen, R. M. (2017). Timing the oxidation of earth's crust: Evidence from big data records of manganese mineralization. In *AGU Fall Meeting Abstracts*, Vol. *24*. Retrieved from http://adsabs.harvard.edu/abs/2017AGUFM.V24C.03H

Johnson, J. W., Oelkers, E. H., & Helgeson, H. C. (1992). Supcrt92 – A software package for calculating the standard molal thermodynamic properties of minerals, gases, aqueous species, and reactions from 1-bar to 5000-bar and 0-degrees-C to 1000-degrees-C. *Computers & Geosciences*, *18*, 899–947.

Klein, C. (2005). Some Precambrian banded iron-formations (BIFs) from around the world: Their age, geologic setting, mineralogy,

metamorphism, geochemistry, and origins. *American Mineralogist*, *90*(10), 1473–1499. https://doi.org/10.2138/am.2005.1871

Korenaga, J.. (2013). Initiation and evolution of plate tectonics on earth: Theories and observations. *Annual Review of Earth and Planetary Sciences*, *41*(1), 117–151. https://doi.org/10.1146/annurev-earth-050212-124208

Korenaga, J., Planavsky, N. J., & Evans, D. A. D. (2017). Global water cycle and the coevolution of the earth's interior and surface environment. *Philosophical Transactions of the Royal Society A: Mathematical, Physical and Engineering Sciences*, *375*(2094), 20150393. https://doi.org/10.1098/rsta.2015.0393

Kump, L. R., & Seyfried, W. E. (2005). Hydrothermal Fe fluxes during the precambrian: Effect of low oceanic sulfate concentrations and low hydrostatic pressure on the composition of black smokers. *Earth and Planetary Science Letters*, *235*(3), 654–662. https://doi.org/10.1016/j.epsl.2005.04.040

Large, R. R., Halpin, J. A., Danyushevsky, L. V., Maslennikov, V. V., Bull, S. W., Long, J. A., … Calver, C. R. (2014). Trace element content of sedimentary pyrite as a new proxy for deep-time ocean-atmosphere evolution. *Earth and Planetary Science Letters*, *389*(March), 209–220. https://doi.org/10.1016/j.epsl.2013.12.020

Lebedel, V., Lezin, C., Andreu, B., Wallez, M.-J., Ettachfini, E. M., & Riquier, L. (2013). Geochemical and palaeoecological record of the cenomanian-turonian anoxic event in the carbonate platform of the preafrican trough, Morocco. *Palaeogeography, Palaeoclimatology, Palaeoecology*, *369*(January), 79–98. https://doi.org/10.1016/j.palaeo.2012.10.005

Lee, C. C., Yilin, H. U., & Ribbe, M. W. (2010). Vanadium nitrogenase reduces CO. *Science*, *329*(5992), 642–642. https://doi.org/10.1126/science.1191455

Littlechild, J., Garcia-Rodriguez, E., Dalby, A., & Isupov, M. (2002). Structural and functional comparisons between vanadium haloperoxidase and acid phosphatase enzymes. *Journal of Molecular Recognition*, *15*(5), 291–296. https://doi.org/10.1002/jmr.590

Liu, C., Eleish, A., Hystad, G., Golden, J. J., Downs, R. T., Morrison, S. M., … Hazen, R. M. (2018). Analysis and visualization of vanadium mineral diversity and distribution. *American Mineralogist*, *103*(7), 1080–1086. https://doi.org/10.2138/am-2018-6274

Luo, G., Ono, S., Beukes, N. J., Wang, D. T., Xie, S., & Summons, R. E. (2016). Rapid oxygenation of earth's atmosphere 2.33 billion years ago. *Science Advances*, *2*(5), e1600134. https://doi.org/10.1126/sciadv.1600134

Lyalkova, N. N., & Yurkova, N. A. (1992). Role of microorganisms in vanadium concentration and dispersion. *Geomicrobiology Journal*, *10*(1), 15–26. https://doi.org/10.1080/01490459209377901

McKenna, C. E., Benemann, J. R., & Traylor, T. G. (1970). A vanadium containing nitrogenase preparation: Implications for the role of molybdenum in nitrogen fixation. *Biochemical and Biophysical Research Communications*, *41*(6), 1501–1508. https://doi.org/10.1016/0006-291X(70)90557-7

Meunier, J. D. (1994). The composition and origin of vanadium-rich clay minerals in Colorado plateau Jurassic sandstones. *Clays and Clay Minerals*, *42*(4), 391–401. https://doi.org/10.1346/CCMN.1994.0420403

Middelburg, J. J., van der Weijden, C. H., & Woittiez, J. R. W. (1988). Chemical processes affecting the mobility of major, minor and trace elements during weathering of granitic rocks. *Chemical Geology*, *68*(3), 253–273. https://doi.org/10.1016/0009-2541(88)90025-3

Miller, R. W., & Eady, R. R. (1988). Molybdenum and vanadium nitrogenases of azotobacter chroococcum. Low temperature favours N2 reduction by vanadium nitrogenase. *Biochemical Journal*, *256*(2), 429–432. https://doi.org/10.1042/bj2560429

Moore, E. K., Jelen, B. I., Giovannelli, D., Raanan, H., & Falkowski, P. G. (2017). Metal availability and the expanding network of microbial metabolisms in the Archaean eon. *Nature Geoscience*, *10*(9), 629–636. https://doi.org/10.1038/ngeo3006

Nesbitt, H. W. (1979). Mobility and fractionation of rare earth elements during weathering of a granodiorite. *Nature*, *279*(5710), 206–210. https://doi.org/10.1038/279206a0

Ortiz-Bernad, I., Anderson, R. T., Vrionis, H. A., & Lovley, D. R. (2004). Vanadium respiration by geobacter metallireducens: Novel strategy for in situ removal of vanadium from groundwater. *Applied and Environment Microbiology*, *70*(5), 3091–3095. https://doi.org/10.1128/AEM.70.5.3091-3095.2004

Pan, Y., & Fleet, M. E. (1992). Mineral chemistry and geochemistry of vanadian silicates in the hemlo gold deposit, Ontario, Canada. *Contributions to Mineralogy and Petrology*, *109*(4), 511–525. https://doi.org/10.1007/BF00306553

Rapp, R. P., & Watson, E. B. (1995). Dehydration melting of metabasalt at 8–32 Kbar: Implications for continental growth and crust-mantle recycling. *Journal of Petrology*, *36*(4), 891–931. https://doi.org/10.1093/petrology/36.4.891

Rehder, D. (2000). Vanadium nitrogenase. *Journal of Inorganic Biochemistry*, *80*(1), 133–136. https://doi.org/10.1016/S0162-0134(00)00049-0

Rehder, D. (2008). Is vanadium a more versatile target in the activity of primordial life forms than hitherto anticipated? *Organic & Biomolecular Chemistry*, *6*(6), 957–964. https://doi.org/10.1039/B717565P

Rehder, D. (2015). The role of vanadium in biology. *Metallomics*, *7*(5), 730–742. https://doi.org/10.1039/C4MT00304G

Reimann, C., & Caritat, P. (1998). *Chemical elements in the environment: Fact sheets for the geochemist and environmental scientist*. Berlin, Germany: Springer-Verlag.

Saito, M. A., Sigman, D. M., & Morel, F. M. M. (2003). The bioinorganic chemistry of the ancient ocean: The co-evolution of cyanobacterial metal requirements and biogeochemical cycles at the Archean-Proterozoic boundary? *Inorganica Chimica Acta*, *356*(December), 308–318. https://doi.org/10.1016/S0020-1693(03)00442-0

Salminen, R., Batista, M. J., Bidovec, M., Demetriades, A., De Vivo, B., De Vos, W., … Tarvainen, T. (2005). *Geochemical atlas of Europe, part 1, background information, methodology and maps*. Geological Survey of Finland. Retrieved from https://bib.irb.hr/prikazi-rad?rad=210450

Schlesinger, W. H., Klein, E. M., & Vengosh, A. (2017). Global biogeochemical cycle of vanadium. *Proceedings of the National Academy of Sciences of the United States of America*, *114*(52), E11092–E11100. https://doi.org/10.1073/pnas.1715500114

Scott, C., Lyons, T. W., Bekker, A., Shen, Y., Poulton, S. W., Chu, X., & Anbar, A. D. (2008). Tracing the stepwise oxygenation of the proterozoic ocean. *Nature*, *452*(7186), 456–459. https://doi.org/10.1038/nature06811

Shearer, C. K., McKay, G., Papike, J. J., & Karner, J. M. (2006). Valence state partitioning of vanadium between olivine-liquid: Estimates of the oxygen fugacity of Y980459 and application to other olivine-phyric martian basalts. *American Mineralogist*, *91*(10), 1657–1663. https://doi.org/10.2138/am.2006.2155

Shilov, A., Denisov, N., Efimov, O., Shuvalov, N., Shuvalova, N., & Shilova, A. (1971). New nitrogenase model for reduction of molecular nitrogen in protonic media. *Nature*, *231*(5303), 460–461. https://doi.org/10.1038/231460a0

Stern, R. J. (2005). Evidence from ophiolites, blueschists, and ultrahigh-pressure metamorphic terranes that the modern episode of subduction tectonics began in neoproterozoic time. *Geology*, *33*(7), 557–560. https://doi.org/10.1130/G21365.1

Sutton, S. R., Karner, J., Papike, J., Delaney, J. S., Shearer, C., Newville, M., … Dyar, M. D. (2005). Vanadium K edge XANES of synthetic and natural basaltic glasses and application to microscale oxygen barometry. *Geochimica et Cosmochimica Acta*, *69*(9), 2333–2348. https://doi.org/10.1016/j.gca.2004.10.013

Sverjensky, D. A., Hemley, J. J., & D'angelo, W. M. (1991). Thermodynamic assessment of hydrothermal alkali feldspar-mica-aluminosilicate equilibria. *Geochimica Et Cosmochimica Acta*, *55*, 989–1004. https://doi.org/10.1016/0016-7037(91)90157-Z

Szalay, A., & Szilágyi, M. (1967). The association of vanadium with humic acids. *Geochimica et Cosmochimica Acta*, *31*(1), 1–6. https://doi.org/10.1016/0016-7037(67)90093-2

Taylor, S. R., & McLennan, S. M. (1995). The geochemical evolution of the continental crust. *Reviews of Geophysics*, *33*(2), 241–265. https://doi.org/10.1029/95RG00262

Trefry, J. H., & Metz, S. (1989). Role of hydrothermal precipitates in the geochemical cycling of vanadium. *Nature*, *342*(6249), 531–533. https://doi.org/10.1038/342531a0

Wever, R., & Hemrika, W. (2001).*Handbook of metalloproteins*. A. Messerschmidt, R. Huber, K. Wieghardt, & T. Poulos (Eds.). Chichester, UK: John Wiley & Sons Ltd.

Wickham, H. (2017). *Tidyverse* (version 1.2.1). R. Tidyverse. Retrieved from http://tidyverse.tidyverse.org

Williams, R. J. P. (1981). The bakerian lecture, 1981 natural selection of the chemical elements. *Proceedings of the Royal Society of London, Series B: Biological Sciences*, *213*(1193), 361–397. https://doi.org/10.1098/rspb.1981.0071

Yang, J., Tang, Y. A., Yang, K., Rouff, A. A., Elzinga, E. J., & Huang, J.-H. (2014). Leaching characteristics of vanadium in mine tailings and soils near a vanadium titanomagnetite mining site. *Journal of Hazardous Materials*, *264*(January), 498–504. https://doi.org/10.1016/j.jhazmat.2013.09.063

Zerkle, A. L., House, C. H., & Brantley, S. L. (2005). Biogeochemical signatures through time as inferred from whole microbial genomes. *American Journal of Science*, *305*(6–8), 467–502. https://doi.org/10.2475/ajs.305.6-8.467

Zerkle, A. L., House, C. H., Cox, R. P., & Canfield, D. E. (2006). Metal limitation of cyanobacterial N2 fixation and implications for the precambrian nitrogen cycle. *Geobiology*, *4*(4), 285–297. https://doi.org/10.1111/j.1472-4669.2006.00082.x

Zheng, Q., Zhang, Y., Liu, T., Huang, J., Xue, N., & Shi, Q. (2017). Optimal location of vanadium in muscovite and its geometrical and electronic properties by DFT calculation. *Minerals*, *7*(3), 32. https://doi.org/10.3390/min7030032

SUPPORTING INFORMATION

Additional supporting information may be found online in the Supporting Information section.

How to cite this article: Moore EK, Hao J, Spielman SJ, Yee N. The evolving redox chemistry and bioavailability of vanadium in deep time. *Geobiology*. 2020;00:1–12. https://doi.org/10.1111/gbi.12375